

# ENPH 453 Advanced Engineering Physics Lab

Lab 1: Photoluminescence (PL)

Report Author: Julia Everitt

Teammates: Claire Floras, Kate Szabo

February 13<sup>th</sup>, 2023

## Executive Summary

The purpose of this experiment was to study the impurities and defects in a semiconductor single crystal using the PL spectroscopic method and compare the optical properties to that of samples in previous literature. We are motivated to study  $\text{CsPbBr}_3$  specifically as it is being investigated for use in high energy radiation detection as a better alternative to current detector materials. The sample used was grown by Prof. Peng Wang's research group in 2021 in Chernoff Hall, using the Vertical Bridgman method.

Power and temperature dependent studies were conducted to gain some understanding of the native defects in the crystal structure. Quantification of the electronic states of these defects was outside the scope of this investigation; instead, properties of the sample used were compared to previous work.

When studying the PL intensity as a function of energy, we expected to see a curve with that can be decomposed into two excitonic peaks at each temperature. Previous studies found these peaks to be centered at 2.29 eV and 2.33 eV. The investigation resulted in peaks at  $(2.2749 \pm 0.0006)$  eV and  $(2.3228 \pm 0.0002)$  eV. Temperature dependent raw and decomposed data is shown in Figure 1.

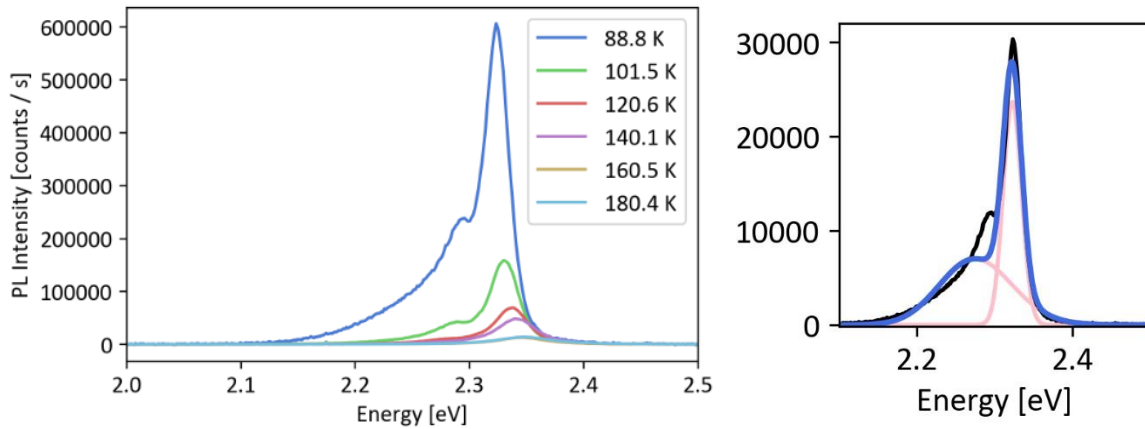


Figure 1: (a) PL intensity vs energy at temperatures ranging from 88.8 K to 180.4 K. (b) The 88.8 K curve decomposed into two Gaussian functions using GaussPy package.

From the temperature dependent study, the phonon energy was determined to be  $(0.04 \pm 0.01)$  eV and the high-temperature activation energies of nonradiative pathways were determined to be  $(0.1 \pm 0.1)$  eV and  $(0.2 \pm 0.2)$  eV. The mean position of the emissions blue shifted with increasing temperatures, which is abnormal since excitonic PL tends to redshift, but was expected based on previous studies.

From the power dependent study, the  $\gamma$  value for the peaks were found to be  $1.9 \pm 0.1$  and  $1.8 \pm 0.1$  for the 2.27 eV and 2.32 eV peaks respectively, confirming both peaks were excitonic emissions.

Results could be improved by using an apparatus with capability to reach lower temperatures. For future studies, this experiment can be extended to study multiple samples and determine optical growth conditions for  $\text{CsPbBr}_3$  based on defect states.

## Abstract

The purpose of this experiment was to study the impurities and defects in a semiconductor single crystal using the PL spectroscopic method and compare the optical properties to that of samples in previous literature. Results showed agreement with previous experiments, indicating the described procedure is well suited for future studies.

$\text{CsPbBr}_3$  is being investigated for use in high energy radiation detection as a better alternative to current detector materials and was the focus of this experiment. The sample used was grown by Prof. Peng Wang's research group in 2021 in Chernoff Hall, using the Vertical Bridgman method. We aimed to study the PL properties of the sample and determine the native defects in the crystal structure, which impact optical properties. Power and temperature dependent studies were conducted.

From the temperature dependent study, the phonon energy was determined to be  $(0.04 \pm 0.01)$  eV using the Toyozawa equation. The high-temperature activation energies of nonradiative pathways were determined to be  $(0.1 \pm 0.1)$  eV and  $(0.2 \pm 0.2)$  eV using the thermal quenching equation. Two excitonic peaks were observed at  $(2.2749 \pm 0.0006)$  eV and  $(2.3228 \pm 0.0002)$  eV using Gaussian Decomposition. The mean position of the emissions blue shifted with increasing temperatures, which is abnormal since excitonic PL tends to redshift, but was expected based on previous studies.

From the power dependent study, the  $\gamma$  value for the peaks were found to be  $1.9 \pm 0.1$  and  $1.8 \pm 0.1$  for the 2.27 eV and 2.32 eV peaks respectively, confirming both peaks were excitonic emissions.

For future studies, this experiment can be extended to study multiple samples and determine optical growth conditions for  $\text{CsPbBr}_3$  based on defect states. Furthermore, the electronic states of the defects can be quantified using density functional theory, which was outside the scope of this experiment.

## Introduction and Theory

Photoluminescence (PL) is the emission of light from a material upon excitation by light energy or photons [1]. It can be used to characterize the properties of semiconductors via PL spectroscopy, a non-destructive, contactless method to determine the quality of single crystals. The excitation initiating PL is typically achieved using a laser beam with energy greater than the bandgap energy pointed at the material. Absorption of the excitation photons results in the formation of electron-hole pairs called excitons [2]. The electrons in the conduction band undergo rapid relaxation to the bandgap minimum, and can then recombine with holes in the valence band resulting in the emission of light. The color and intensity of the PL depends on the bandgap energy, the type of semiconductor, and the quality of the crystal structure.

In an ideal semiconductor, the electron-hole recombination occurs due to band-to-band recombination and is associated with bandgap energy [1]. The presence of native and extrinsic defects impacts several properties of real semiconductors, with optical properties being of the most interest to this experiment.

Semiconductors have unique PL properties due to their electronic structure, which is characterized by a bandgap energy that separates the valence and conduction bands [3]. Bandgap energy determines the energy required to excite electrons from the valence band to the conduction band, and the subsequent emission of light upon recombination of the excited electrons with holes in the valence band. Bandgap energy for different materials is illustrated in Figure 2.

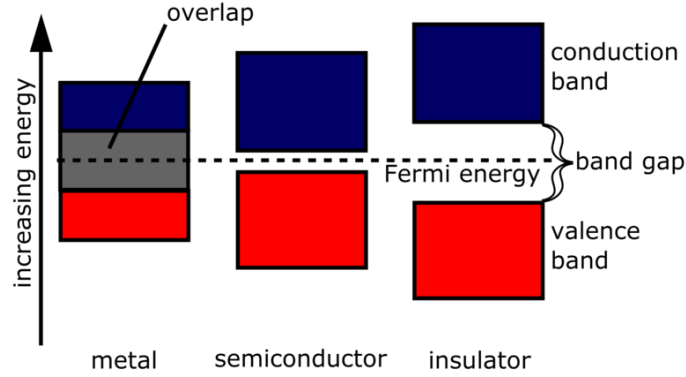


Figure 2: Diagram of the valence band, conduction band, and band gap for semiconductors in contrast to metals and insulators [3].

The Toyozawa equation describes FWHM as a function of temperature and can be used to determine the energy of the phonon,  $E_{ph}$ .

$$\omega(T) = \frac{A}{\exp\left(\frac{E_{ph}}{K_B T}\right) - 1} \quad (1)$$

The thermal quenching equation describes PL intensity as a function of temperature and can be used to determine the high- and low-temperature activation energies of nonradiative pathways, denoted  $E_1$  and  $E_2$ .

$$I(T) = \frac{I_0}{1 + C1 * \exp\left(-\frac{E_1}{K_B T}\right) + C2 * \exp\left(-\frac{E_2}{K_B T}\right)} \quad (2)$$

Since the apparatus does not allow for temperatures below 77 K, the second exponential term can be dropped. Laser power intensity is calculated using Equation 3,

$$I = I_0 * 10^{-(ND)} \quad (3)$$

Where  $I_0 = 3.49 \pm 0.05$  mW for this experiment and ND is the filter. PL intensity is related to the laser intensity by  $PLI \propto L^\gamma$ . A value of  $\gamma$  less than 1 indicates a non-excitonic peak and a value of  $\gamma$  between 1 and 2 indicates an excitonic peak [1].

A better understanding of the PL properties of semiconductors can lead to the development of more efficient and versatile optoelectronic devices for various applications. By studying PL of multiple samples, one could draw conclusions on how different growing techniques impact the quality of the crystals for optimization.

## Apparatus and Procedure

### Apparatus

PL spectroscopy is conducted at cryogenic temperatures due to the small binding energies of the states involved. To achieve this, the apparatus features a cold finger cryostat where the sample is in a vacuum and the top of the cryostat allows liquid nitrogen to be poured in the funnel. A vacuum is created by

connecting a pump with PVC tubing to the chamber. Several samples are mounted with Apiezon N thermal grease to eliminate the need to change samples; instead, slight realignment allows for the study of different samples. The samples are visible through a quartz window, which is transparent in a wide range of wavelengths and suitable for the low temperature and vacuum.

For the excitation, a blue laser pointer with a wavelength of 405 nm and measured intensity of  $3.49 \pm 0.05$  mW is used. The laser beam is guided through a filter, reflects off a mirror to hit the sample in the chamber, then off a parabolic mirror to a focusing lens and fiber coupler to a Flame Mini Spectrometer and LabVIEW program. The apparatus is shown in Figure 3.

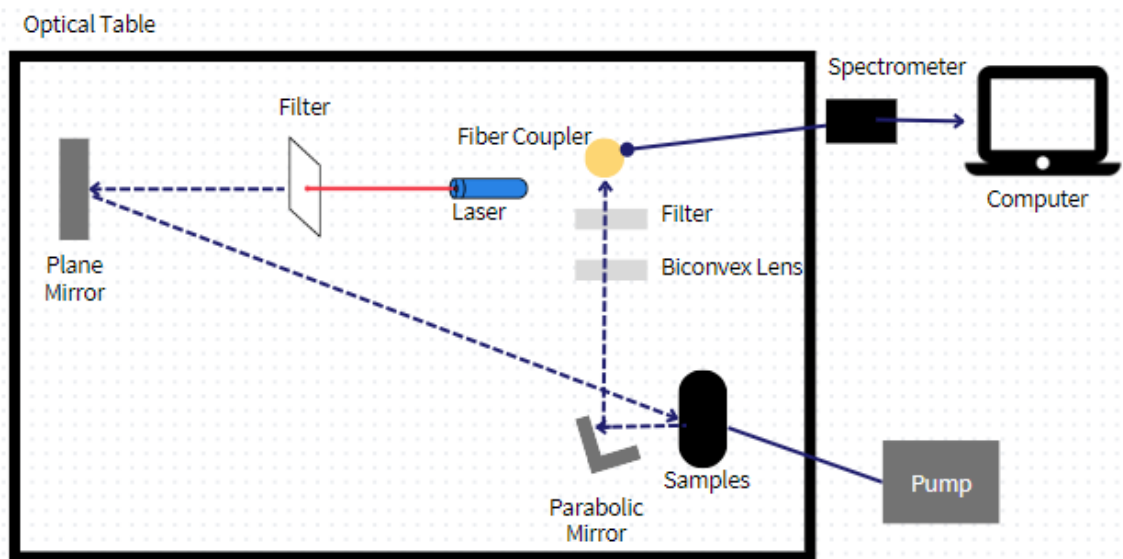


Figure 3: Diagram of apparatus. The laser beam passes through a filter then reflects off of a plane mirror onto the sample. The luminescence is collimated off the parabolic mirror before passing through a focusing lens into the fiber coupler, where it finally goes to the spectrometer and is monitored through LabVIEW on the computer.

The technique described is known as the off axis parabolic mirror technique, which is advantageous over alternatives in that it eliminates errors due to chromatic aberrations.

## Procedure

The experimental procedure is as follows:

1. Place the laser, plane mirror, and sample in approximate positions based on Figure 3. Put on protective eyewear rated in the 400 nm range.
2. Turn on the laser and adjust the plane mirror until the beam exiting the laser is directed onto the  $\text{CsPbBr}_3$  sample. A piece of white paper can be used as an aid while positioning the laser as it is important to avoid direct eye contact. The lights in the room should be turned off as well to make the laser beam more visible. The sample will 'glow' when aligned.
3. Once the laser beam is hitting the sample and you are satisfied with the alignment, turn off the laser, turn on the light, and secure each component to the optical table using the appropriate screws.
4. Turn on the pump to evacuate the chamber.
5. Launch LabVIEW to monitor the temperature of the sample. Pour liquid nitrogen from the primary container into a smaller container, then to the top of the cold finger until it is nearly full.

Note that excessive “bubbling” is to be expected as the components cool down. Continue to add liquid nitrogen as it evaporates until the temperature stabilizes at a minimum value of approximately 88 K.

6. Turn the light in the room off and the laser on. At this point, the PL emission should be visible as a green glow through the quartz window. Adjust the position of the parabolic mirror at the opening of the cryostat window, such that the reflection is collimated and circular. The mirror has a focal length of 3 cm, so it should be very close to the window. Use a piece of paper to observe the reflection as you make adjustments.
7. Place the biconvex lens directly in the path of the luminescence, again using a piece of paper. Fine tune the position of the lens until the smallest PL spot possible is obtained
8. Place the filter in between the laser and plane mirror and. Note that an ND filter should always be used once alignment is achieved to avoid burning the sample.
9. Place the fibre coupler so that the spot is positioned exactly at the opening of the collimator. Make small adjustments to the position and angle of the coupler to increase the amplitude of the peak captured by the spectrometer. If necessary, adjust the integration time of the spectrometer so that the PL peak is well defined, but is not saturating the spectrometer. The integration time describes the time the intensity is measured over.
10. Vary the temperature of the sample or laser power as you collect data depending on what you would like to study, described in the next section. Be sure to give your output data files descriptive names.

## Data Collection

Temperature dependent and power dependent PL studies were conducted. For collection of both of these datasets, the procedure described in the previous section was followed to set up. All measurements must be made without changing the optical alignment to achieve consistent results. Changes in the position of the parabolic mirror, biconvex lens, or coupler could affect the intensity read by the spectrometer.

### Power Dependent PL Study

The laser power was varied by changing the ND filter placed in front of the laser. Filters with ND values of 0.3, 0.6, 0.9, 1.2, and 1.5 were used, with powers given by Equation 3. At each power, the spectrometer readings were recorded in addition to the filter value, temperature, and integration time. The temperature was held constant at the minimum of 88.8 K for each measurement in the power dependent study. Intensity data as a function of laser power is seen in Figure 4.

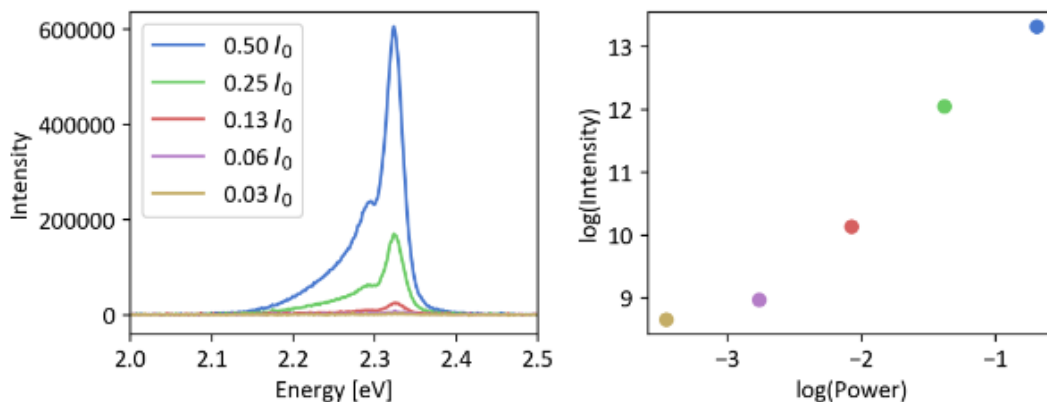


Figure 4: Raw data from power dependent study. The plot on the left shows intensity vs energy for 5 different filters, and the plot on the right shows a linear relationship between intensity and power on log-log scale.

### Temperature Dependent PL Study

For the temperature dependent PL study, the filters ND=0.3, 0.6, and 0.9 were used as they gave the least noisy data. For each of these three filters, the spectrometer readings in addition to the temperature and filter were recorded at the lowest temperature of 88.8 K. This was repeated after waiting for the temperature to increase to 100 K, then at 20 K increments from 120 K to 180 K. Temperature increased at a rate of  $\sim 0.02$  K per second. A plot of the PL spectra as a function of wavelength for  $T=88.8$  K using filter ND=0.3 is seen in Figure 5.

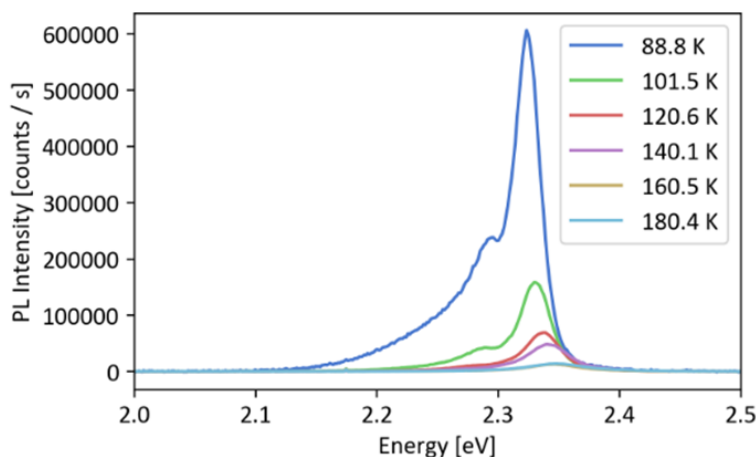


Figure 5: PL Intensity vs Wavelength for ND=0.3 filter. Uncertainty in the wavelength is 0.19 nm before conversion to energy and uncertainty in intensity is the square root of the value. Beyond 180 K the signal becomes too weak to meaningfully observe.

The data using ND=0.3 exhibited the clearest peaks and was therefore used for analysis going forward. The plots for the other filters can be seen in the appendix.

Note that the PL intensity measurements represent the number of emission counts per second at a given wavelength. Intensity is often used interchangeably with amplitude in this report.

## Data Analysis

### Gaussian Decomposition

Gaussian decomposition was performed to separate the curves shown in FIGURE XX into two gaussians for further analysis. The two peaks represent bound excitonic luminescence peaks, as expected to see. Analysis in [Power Dependent Study] confirms the excitonic nature of these peaks. An example of a decomposed plot is seen in Figure 6 below: the single peak at approximately 2.31 eV decomposes into two peaks centered at  $(2.2749 \pm 0.0006)$  eV and  $(2.3228 \pm 0.0002)$  eV. The uncertainty in wavelength is half of the smallest division, which is a constant 0.19 nm which was then converted to be in terms of energy. The uncertainty in the amplitude is the square root of the intensity. These errors are propagated through the decomposition model to give resultant errors on all output values.

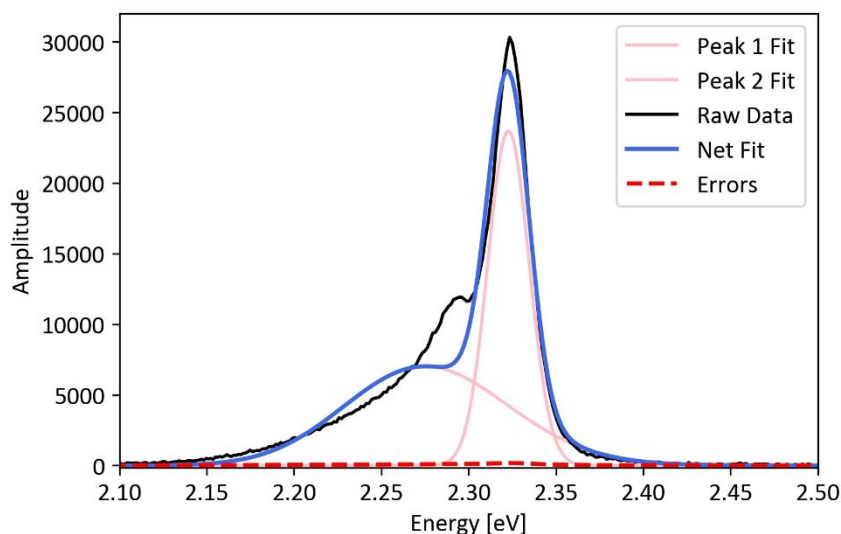


Figure 6: Gaussian decomposition results for  $T=90$  K,  $ND=0.3$  data with the x-axis in terms of energy. Peaks are seen at  $(2.2749 \pm 0.0006)$  eV and  $(2.3228 \pm 0.0002)$  eV. The black curve is the raw data, the pink curves are the two gaussian fits, and the blue curve is the net fit, which is the sum of the two pink curves. The red line is the uncertainty of the amplitude, which is the square root of the amplitude. The uncertainty in energy comes from a wavelength uncertainty of 0.19 nm.

To achieve this fit, GaussPy was used – a free, open-source Gaussian Decomposition Tool written in Python available through GitHub [4]. To make our data compatible with GaussPy, it was first converted to pickle format, which serializes the data for efficient loading and saving. Hyperparameters were then fine-tuned to achieve a suitable fit, and results were plotted to confirm. GaussPy returns the fitted mean position, amplitude, full width half maximum (FWHM) for each peak. The uncertainties from experimental data are propagated to give error values on each of these.

This decomposition process was conducted to determine the mean position, amplitude, and FWHM for the temperature dependent study in addition to the amplitudes for the power dependent study. The alpha and signal-to-noise ratio (SNR) hyperparameters must be adjusted to achieve a suitable fit for each temperature and power variation, making the process manual and time consuming. IGOR Pro paid software has been used in the past and is a more user friendly and accurate option.



### Power Dependent PL Study

The power dependent PL study was conducted to determine whether the luminescence peaks were excitonic or non-excitonic. Laser power was plotted against intensity on log-log scale, shown in Figure 7.

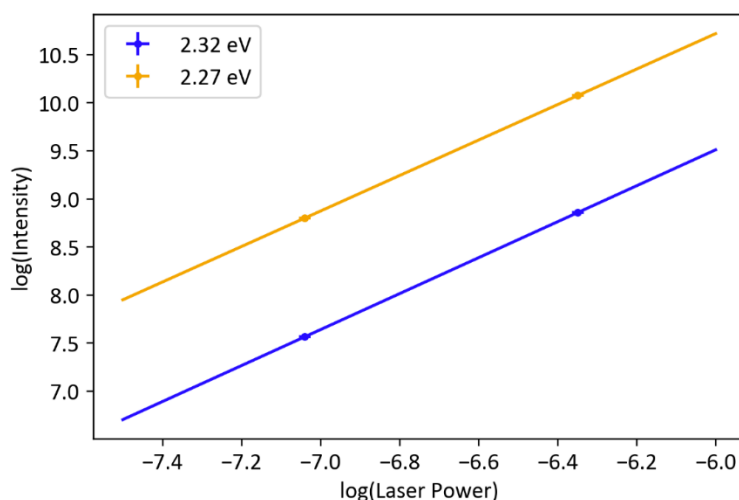


Figure 7: Laser power plotted against PL intensity on a log-log scale. X and Y error bars are included. The slope of the lines are  $1.9 \pm 0.1$  and  $1.8 \pm 0.1$  for the 2.27 eV and 2.32 eV peaks respectively, indicating excitonic emissions.

The two points on the graph represent the intensity of the two peaks using ND=0.3 and ND=0.6 filters. Gaussian decomposition was unsuccessful for the filters with higher ND values. Uncertainty of the laser power comes from the initial intensity,  $I_0 = (3.49 \pm 0.05)$  mW, and uncertainty in intensity is the square root of the value, propagated through GaussPy. The uncertainty on the slopes of  $1.9 \pm 0.1$  and  $1.8 \pm 0.1$  for the 2.27 eV and 2.32 eV peaks was calculated by determining the maximum and minimum values from uncertainty in raw data.

### Temperature Dependent PL Study

Uncertainty in temperature for this section was based on the observed average temperature change of the apparatus, which was 0.02 K per second multiplied by the integration time. This represents the change in the temperature of the sample over the measurement time.

#### Mean Position vs Temperature

Using the GaussPy results, the mean position of each peak was plotted as a function of temperature, seen in Figure 8 below.

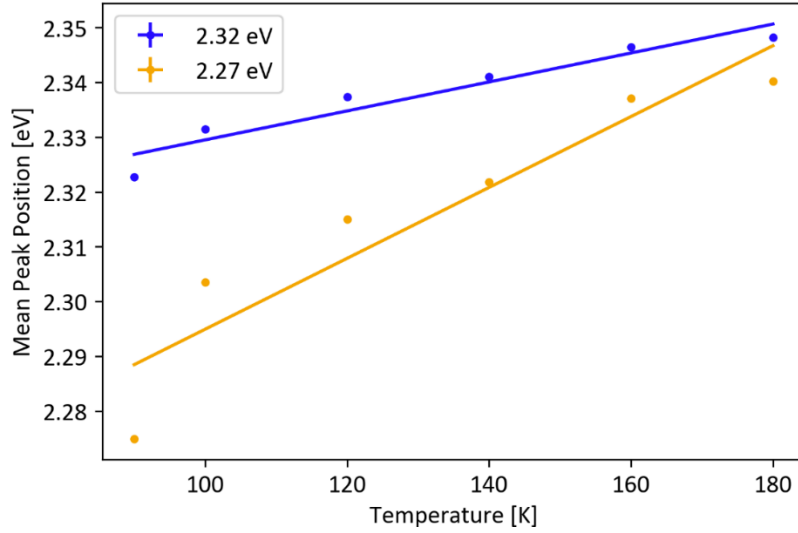


Figure 8: Mean peak position as a function of temperature for the decomposed PL peaks with error bars. A positive linear relationship is seen as expected from literature, indicating a blueshift with increasing temperature.

### FWHM vs Temperature

FWHM was plotted as a function of temperature seen in Figure 9, and was fit using the Toyozawa equation to determine the energy of the phonon,  $E_{ph}$ .

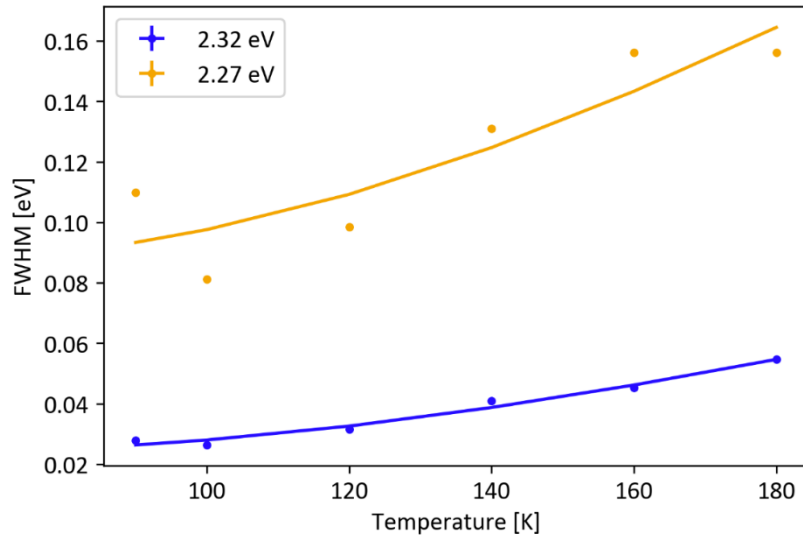


Figure 9: FWHM of the 2.32 eV and 2.27 eV peaks as a function of temperature. X and Y errors are included.

The data was fit to the Toyozawa equation, Equation 1, to determine  $E_{ph}$ , the energy of the phonon. Scipy Curve Fit was used for this. This resulted in phonon values of  $(0.04 \pm 0.01)$  eV and  $(0.04 \pm 0.05)$  eV.

### Intensity vs Temperature

Thermal quenching of the PL intensity was analyzed to determine high-temperature activation energy of nonradiative pathways. Figure 10 shows the data and fit, found using Scipy Curve Fit with Equation 2.

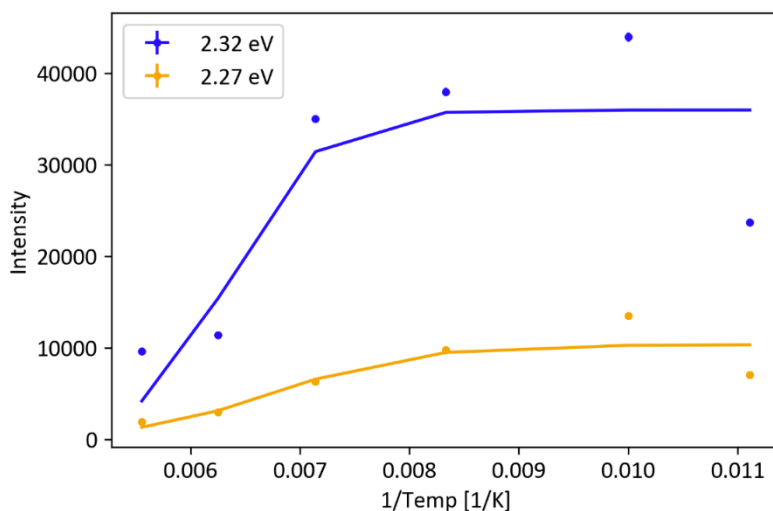


Figure 10: PL intensity plotted against inverse temperature. The fit generated using the thermal quenching equation for each peak is displayed.

## Results and Discussion

### Power Dependent PL Study

The slopes of the laser power vs intensity graph are  $1.9 \pm 0.1$  and  $1.8 \pm 0.1$  for the 2.27 eV and 2.32 eV peaks respectively. Since the slopes are between 1 and 2, this suggests both peaks are excitonic, as expected. Previous work saw slopes of 1.5 and 1.4 for the lower and higher energy peaks respectively, which is in approximate agreement with our observations [5]. The excitonic peaks can be attributed to recombination involving Br vacancy centers [5].

This study was limited by the temperature range of the apparatus as at the minimum temperature of 88.8 K, we could only accurately decompose the gaussian curves for the two lowest filters of ND=0.3 and ND=0.6. The slope was therefore calculated using only two points. Since the curve flattens out for lower laser intensity, we would expect the slope to decrease and more closely match the predicted values of 1.5 and 1.4 if we could fit with more data points. This could be achieved if the temperature of the apparatus could have been lower, or with better decomposition software.

### Temperature Dependent PL Study

Previous studies indicate that a CsPbBr<sub>3</sub> single crystal exhibits emission peaks centered at 2.29 eV and 2.33 eV at a temperature of 10 K. Our measured peaks centered at  $(2.2749 \pm 0.0006)$  eV and  $(2.3228 \pm 0.0002)$  eV at a temperature of 88.8 K agree with this.

The phonon energy was determined to be  $(0.04 \pm 0.01)$  eV using the Toyozawa equation. Previous studies found a phonon energy of 0.016 eV, about half of our value. This discrepancy is likely due to our lack of data points at low temperatures. Since the FWHM vs T curve is flat at temperatures below 50 K, a more representative dataset over a full range of temperatures should yield a phonon energy that matches literature.

The high-temperature activation energies of nonradiative pathways were determined to be  $(0.1 \pm 0.1)$  eV and  $(0.2 \pm 0.2)$  eV using the thermal quenching equation. A previous study found a value of 0.017 for the net curve, about 10 times less than our measurement. The difference is likely due to our lack of

measurements at low temperature and the native defects specific to our sample. Note that our analysis considered the two emission peaks separately rather than the net curve, which was used for the phonon energy and activation energy calculations in the previous study.

The mean position of the emission peaks blue shifted with increasing temperatures. Typically, a red shift is seen in semi conductor because the bandgap shrinks with increasing temp. Our observation of a blue shift confirms the presence of defect states. This effect was also seen in previous studies.

Measured and calculated values agreed with past studies within reason, other than the activation energies of non-radiative pathways, which were found to be 10 times larger than expected. This discrepancy was attributed to a lack of data points at sufficiently low temperature, the primary limitation.

## Conclusion

We set out in this investigation to study the native defects of single crystal  $\text{CsPbBr}_3$ . Although we were unable to quantify the electronic states of the defects or compare multiple samples, we collected accurate data that confirms results from previous studies and demonstrates the viability of this technique for future studies.

We found that the  $\text{CsPbBr}_3$  sample exhibited two excitonic peaks centered at  $(2.2749 \pm 0.0006)$  eV and  $(2.3228 \pm 0.0002)$  eV at a temperature of 88.8 K and laser intensity of  $3.49 \pm 0.05$  mW. The excitations were above band gap excitations because the emission has lower energy than the incident laser. The phonon energy was determined to be  $(0.04 \pm 0.01)$  eV, the high-temperature activation energies of nonradiative pathways were determined to be  $(0.1 \pm 0.1)$  eV, and the position of the emission peaks blue shifted with increasing temperatures due to phonon assisted processes.

## References

- [1] S. Kostina, "Photoluminescence of Semiconductors," Kingston, 2022.
- [2] K. K. Smith, "Photoluminescence of semiconductor materials," *Thin Solid Films*, vol. 84, pp. 171-182, 1981.
- [3] "Energy Education," [Online]. Available: [https://energyeducation.ca/encyclopedia/Band\\_gap](https://energyeducation.ca/encyclopedia/Band_gap).
- [4] GaussPy, "GaussPy," 2021. [Online]. Available: <https://github.com/gausspy/gausspy/tree/master/gausspy>. [Accessed February 2023].
- [5] M. S. e. Al, "Excitonic emissions and above-band-gap luminescence in the single-crystal perovskite," 2015.

## Appendix

Figure 11 shows additional intensity vs energy plots excluded from the Data Collection section.

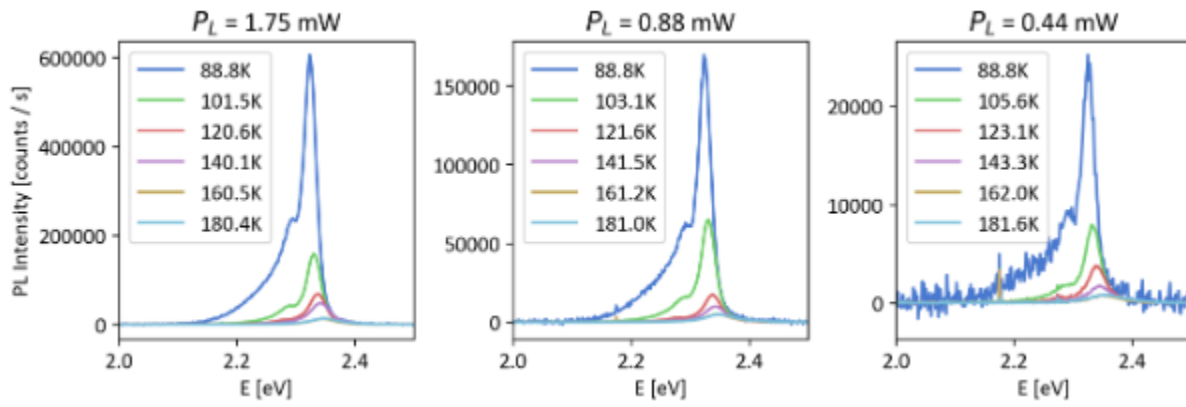


Figure 11: Additional intensity vs energy plots for 3 different laser intensities, corresponding to filters ND=0.3, 0.6, and 0.9.